Glacier microseismicity

Michael E. West[1], Christopher F. Larsen[1], Martin Truffer[1], Shad O'Neel[2], and Laura LeBlanc[1]
[1]Geophysical Institute, University of Alaska Fairbanks, Fairbanks, Alaska 99775, USA
[2]Water Resources Division, U.S. Geological Survey, Anchorage, Alaska 99508, USA

ABSTRACT

We present a framework for interpreting small glacier seismic events based on data collected near the center of Bering Glacier, Alaska, in spring 2007. We find extremely high microseismicity rates (as many as tens of events per minute) occurring largely within a few kilometers of the receivers. A high-frequency class of seismicity is distinguished by dominant frequencies of 20–35 Hz and impulsive arrivals. A low-frequency class has dominant frequencies of 6–15 Hz, emergent onsets, and longer, more monotonic codas. A bimodal distribution of 160,000 seismic events over two months demonstrates that the classes represent two distinct populations. This is further supported by the presence of hybrid waveforms that contain elements of both event types. The high-low-hybrid paradigm is well established in volcano seismology and is demonstrated by a comparison to earthquakes from Augustine Volcano. We build on these parallels to suggest that fluid-induced resonance is likely responsible for the low-frequency glacier events and that the hybrid glacier events may be caused by the rush of water into newly opening pathways.

MOTIVATION

Studies of glacier seismicity span at least four decades. A handful of pioneering studies focused on crevassing (Neave and Savage, 1970; Deichmann et al., 1979), the source of enigmatic regional seismicity (Van Wormer and Berg, 1973; Weaver and Malone, 1979; Wolf and Davies, 1986), the seismic signature of iceberg calving (Qamar, 1988), and friction at the rock-ice interface (Anandakrishnan and Bentley, 1993; Anandakrishnan and Alley, 1994; Smith, 2006). There has been a surge in glacier seismology in the past few years driven, in part, by the recognition of globally recorded "glacial earthquakes" (Ekström et al., 2003; Wiens et al., 2008) and their apparent relationship to climate change (Ekström et al., 2006). Recent projects to address this connection have been pursued in Alaska (Larsen et al., 2007), Greenland (Amundson et al. 2008; Nettles et al., 2008), the Alps (Walter et al., 2008), and Antarctica (Wiens et al., 2008). These studies examine glacier dynamics on several scales, from microseismicity recorded within a few kilometers of the source, to events observed on regional networks, to teleseismically recorded glacier earthquakes. Here we focus on microseismicity typically recorded within a few kilometers of the source that can occur at rates as high as tens of events per minute.

We propose that some paradigms for understanding glacier microseismicity may be drawn from the long history of seismic applications at volcanoes. The two environments are analogous on several levels. Both are characterized by pressurized fluid phases moving through, and interacting with, a solid matrix that may locally be near its solidus temperature. In glaciers, this interaction is between ice and water. In volcanoes, the matrix is rock and the fluids are gas, magma, and water. St. Lawrence and Qamar (1979) specifically noted similarities between low-frequency glacier and volcano waveforms recorded on regional seismic arrays. Here we apply a similar idea to microseismicity and demonstrate that the high- and low-frequency event classification scheme used extensively in volcano seismology is quantitatively valid in a glacier setting as well. We also describe for the first time a class of hybrid glacier seismic events that exhibits both types of behavior in rapid succession.

BERING GLACIER EXPERIMENT

Bering Glacier flows from the St. Elias mountain range to its terminus on the south-central coast of Alaska (Fig. 1). It is a temperate glacier, with the ice near its melting point throughout, with a history of dramatic surges (Molnia and Post, 1995). In the spring of 2007 five seismic stations were deployed halfway between the terminus and the equilibrium line altitude, several tens of kilometers from either. During the study period, the stations consisted of three-component Mark Products L22 short-period seismometers recorded on Quanterra Q330 dataloggers at 200 samples/s. Two sites had collocated three-component Guralp CMG-6TD broadband (30 s) seismometers (Larsen et al., 2007). The cross-shaped seismic array had an aperture of 4 km and was located near the central flow line, where the glacier is 10 km wide and ~700 m thick (Conway et al., 2009). Surface features and crevasses observed at the

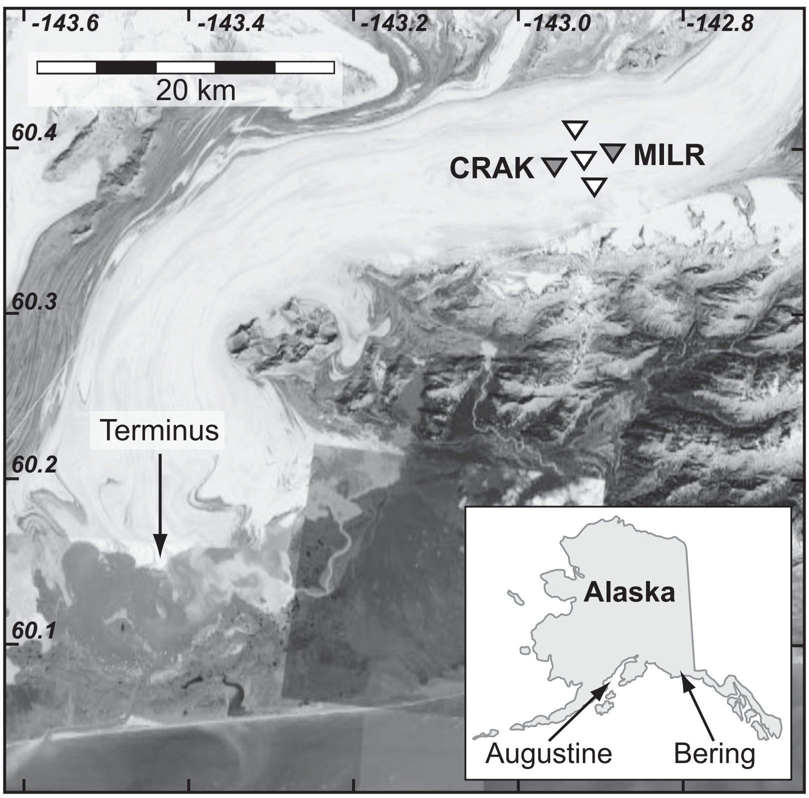

Figure 1. Map of lower Bering Glacier experiment overlain on Landsat imagery. Triangles mark locations of seismic stations.

deployment site are representative of the glacier's ablation area.

The environment proved to be extremely seismically active, often registering seismic events every few seconds. Visual inspection of the network data demonstrates that events arrive from all directions inside and outside of the network. Accurate locations are generally not possible due to limited station coverage. However, surface wave to body wave amplitude ratios suggest that events come from both the shallow and deep portions of the ice. The source properties are equally varied: impulsive and emergent; long and short codas; dominated by body waves and surface waves; and frequency contents that vary by more than an order of magnitude. The tremendous range of event types complicated initial efforts to characterize the data set and attempts to tie ice motion to seismicity (Larsen et al., 2007). Schemes that characterized events by their frequency content not only proved successful, but also suggested that there is a physical basis for distinguishing events by frequency.

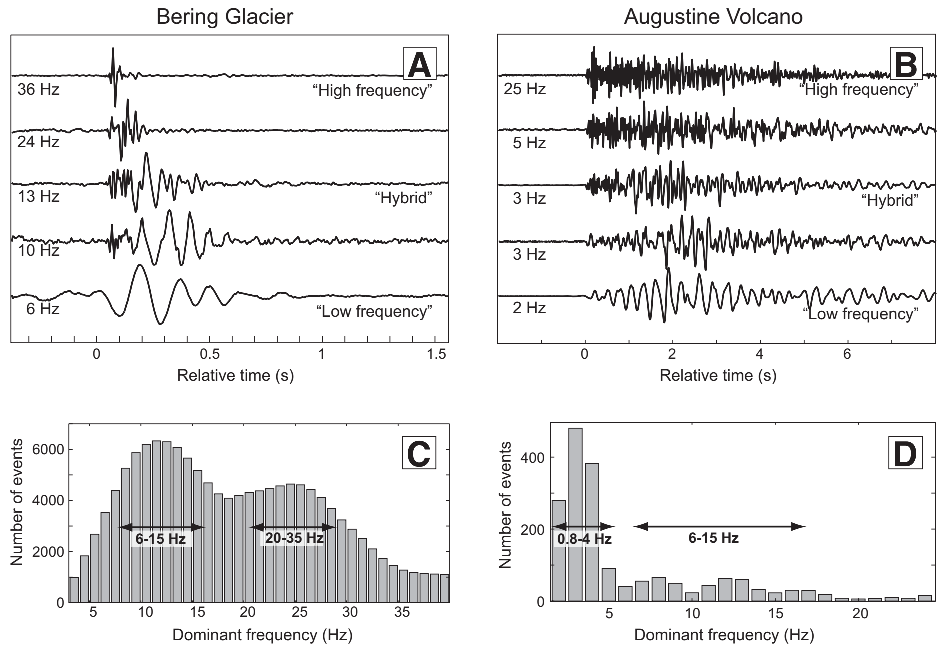

Figure 2. Seismic event classes from Bering Glacier and Augustine Volcano. A: Sample waveforms from Bering Glacier. Dominant frequencies are shown along left side. B: Sample waveforms from Augustine Volcano. C: Distribution of dominant frequencies at Bering Glacier. D: Distribution of dominant frequencies at Augustine Volcano.

GLACIER MICROSEISMICITY

Glacier microseismicity was detected using a standard short-term average to long-term average (STA/LTA) detection algorithm operating in three overlapping frequency bands (0.8–5 Hz, 3–20 Hz, and 8–50 Hz). By requiring a signal-to-noise ratio >10, we ignore all but the highest quality events. Using the vertical channel of station CRAK these criteria yielded 160,000 events between 20 April and 19 June 2007, with a mean detection interval of 30 s. Visual inspection shows that more than 98% of the detections correspond to the first arrival of seismic events with durations <2 s. The events comprise a wide range of waveforms and frequency contents (Fig. 2A). The bulk of these events are observed only weakly on adjacent seismic stations, suggesting source to receiver distances less than the station spacing (2 km).

For each event, we extract a 2 s window of data beginning 0.4 s before the detection time. Traces are high-pass filtered above 0.8 Hz and then prepared with a cosine taper at each end. After a transformation to the frequency domain, we find the frequency with the most energy. This dominant frequency appears robust to processing parameters. We use it here as a proxy for the overall frequency content of the waveform.

The dominant frequencies show a bimodal distribution with concentrations centered between 6 and 15 Hz and 20–35 Hz (Fig. 2C). The same pattern is observed for data from station MILR and for subsets within the two-month period, though the proportion of high- to low-frequency events is quite variable. Because we make no attempt to correct for the source distance, the distribution of frequencies is affected by attenuation. Attenuation within the ice will remove high frequencies from the waveforms at a faster rate than low frequencies. While this will tend to shift energy lower on the frequency spectra, attenuation will not create the bimodal distribution. The two peaks in the frequency distribution suggest two separate source processes. This high-frequency/low-frequency paradigm parallels a long-standing classification applied to volcanic earthquakes (next section).

Seismicity from crevassing is well observed in many glacier settings (e.g., Neave and Savage, 1970; Walter et al., 2008). Frequencies of brittle failure quakes scale by the size of the fault and, to a lesser degree, the shear modulus of the medium. Estimates of rupture size are complicated by unknown attenuation characteristics and the lack of source locations. However, based on the propagation distances of just a few kilometers and in situ observations elsewhere, we infer rupture displacements measurable in centimeters (Walter et al., 2008).

A class of low-frequency fluid-sourced seismicity has a conceptual appeal, especially in temperate ice where pockets of water may be numerous and long-lived. Meteoric and meltwater drain into the ice from the surface. High-pressure water fills englacial voids and flows along the base of the glacier. This is particularly true for temperate glaciers, such as Bering, in marine climates where high rates of precipitation and ablation lead to high mass turnover. Ablation at the site of the network was measured at 4.5 m water equivalent per year. A fluid resonant source is further suggested by the presence of narrow peaks in a small number of the low-frequency event amplitude spectra. This concentration of energy in narrow spectral bands is a distinguishing feature of resonant systems, where the characteristic frequency is a function of the resonator dimensions. Harmonic events with extended codas have been documented during surges on the Bakaninbreen glacier (Stuart et al., 2005). These events are interpreted as resonance in water-filled fractures at the base of the surge front. Walter et al. (2008) demonstrated that basal seismic events on the Gornersee glacier were modulated by changes in water pressure, though it should be noted that it was pressure minima they associated with the seismic events in their study. These examples demonstrate the close, though complex, relationship between water and seismic activity on glaciers.

COMPARISON WITH VOLCANO MICROSEISMICITY

Brittle failure earthquakes at volcanoes are indistinguishable from other tectonic earthquakes. They have impulsive onsets, clear P and S waves, and wide frequency content up to 10–20 Hz (McNutt, 2005). Swarms of volcano-tectonic, or high-frequency, events may be caused by stress changes resulting from magma movement, regional tectonics, thermal expansion, and gravitational loading. They can usually be modeled with double-couple source mechanisms (e.g., Roman et al., 2006), though some events require an expansion component often attributed to the injection of pressurized fluid (e.g., Julian et al., 1997).

A second class of volcanic earthquakes is characterized by emergent onsets, the absence of distinct S wave arrivals, and monotonic codas that decay slowly. These events are referred to as low-frequency earthquakes. They are typically rich in frequencies below 5 Hz and often have a dominant spectral peak and harmonics suggesting a resonant source. Several source mechanisms have been proposed (e.g., Julian, 1994; Chouet, 1996; Nakano et al., 1998; Neuberg and O'Gorman, 2002; Fujita and Ida, 2003), all based on the interaction of fluid with the surrounding rock.

A third class of earthquakes shares elements of both high- and low-frequency events (McNutt, 2002). These events, termed hybrids, have high-frequency onsets, but are followed by extended codas of lower-frequency energy. Hybrid events are critical because they provide a link between the mechanisms of the high- and low-frequency earthquakes. Together they implicate a source in which an initial fracture (such as cracking) initiates a fluid resonance through reverberation, bubble coalescence, or turbulent flow.

Figures 2B and 2D illustrate the differences between these events using data from the 2006 eruption of Mount Augustine in Alaska. We use the Augustine eruption because it provides a self-contained example of different waveform classes supported by a full complement of geological and geophysical data streams. The data set includes 1941 handpicked earthquakes from 1 January through 26 January 2007 spanning precursory, explosive, and effusive activity at the volcano (Buurman and West, 2010). Here we show data recorded on broadband station AU13 located 1.8 km south of the Augustine summit. The dominant frequencies of the events fall into two ranges approximately spanning 0.8–4 Hz and 6–18 Hz (Fig. 2C). Representative waveforms of each class are shown in Figure 2B. Buurman and West (2010) demonstrated that the precursory buildup to the eruption was characterized by high-frequency earthquakes as gas or magma opened pathways to the surface. The first ash-rich eruptions were preceded by several hours of hybrid events, suggesting that magma was working its way through the crack pathways toward shallower depths. Low-frequency earthquakes were mostly recorded during the effusive phase as magma was pumped toward the surface through existing conduits. While more nuanced interpretations are possible, the Augustine example nicely illustrates the connection of high-frequency events with brittle fracture and the low-frequency events and hybrids with fluids.

GLACIER HYBRID EVENTS

Dominant frequency is a crude tool and subject to site effects and attenuation. A similar three-class taxonomy for glacier microseismicity is confirmed, however, by the presence of hybrid glacier events. Hybrid events are widely observed in the Bering data set. These waveforms stand out because of the high-frequency impulsive onset that transitions to a lower frequency extended coda (Fig. 2B). Like their volcano counterparts, the first portion of a hybrid glacier event is indistinguishable from the high-frequency class, while the latter portions are identical to the low-frequency events. An attempt to rigorously count hybrid events is challenging because they span a wide variety of waveform types and may fall into either the high or low dominant frequency class. Buurman and West (2010) used ratios of high- and low-frequency energy to classify hybrid events at volcanoes; however, a precise definition remains subjective. Neuberg et al. (2000) demonstrated that there is a continuum between low-frequency and hybrid volcanic earthquakes. The range of intermediate waveforms in Figure 2A suggests that a similar continuum likely exists for glacier hybrids.

Hybrid events are arguably the strongest evidence for two styles of glacier source mechanisms. The distinct sequence of impulsive high-frequency onset followed by an extended low-frequency coda argues for two source mechanisms joined in a single set of events. Mechanisms for the low-frequency class of volcanic events are still debated and probably include more than one. The present analysis is insufficient to bear out a single source for hybrid and low-frequency glacier events. One model is hydrofracturing of the glacier ice. As pooled surface waters penetrate down into the glacier, water pressure drives the progressive expansion of existing cracks (Metaxian et al., 2003; Van Der Veen, 1998; O'Neel and Pfeffer, 2007). High-frequency cracking is followed immediately by the rush of water into the new opening. In this scenario, water pressure drives cracking and seismicity. In an alternative model, cracking is driven by the existing glacier stresses (Walter et al., 2008). Because temperate glaciers are often water saturated, voids created by new fissures can only be filled by water. In this model, water does not drive cracking; however, it is drawn in to fill the void concurrent with the fracturing. Resonance of these fissures or the reservoirs from which the water is sourced seems the most viable explanation for the low-frequency events. If this is true, then hybrid events are merely those low-frequency events that are initiated by high-frequency cracking. These simple models are not constrained by the current data. We hope it will provide a starting point for further exploration of low-frequency and hybrid glacier events.

TIME HISTORY OF EVENT TYPES

The different types of microseismicity are important because they imply different glacier dynamics. Based on the wide variety of seismicity already observed across many glacier settings (see Motivation discussion for examples), we hypothesize that these three event classes can be found at most glaciers, though with highly variable rates. The relative proportions of each class will vary substantially in wet and dry glaciers, with more low-frequency events in water-saturated temperate glaciers. If this expectation proves true, it will lend credence to the fluid-driven low-frequency hypothesis.

The most exciting prospect may be tracking the event classes through time to observe transient phenomena. Based on Figure 2C, we divide into subsets the events with dominant frequencies of 6–15 Hz and 20–35 Hz. Figure 3 shows the daily event rate of the low- and high-frequency classes as recorded on station CRAK. Both event types show a dramatic increase beginning on 5 May. This is presumably tied to the spring speed-up of the glacier. Spring speed-up is a widely observed phenomenon in temperate glaciers thought to be triggered by the increased flux of meltwater (Willis, 1995). Over the following six

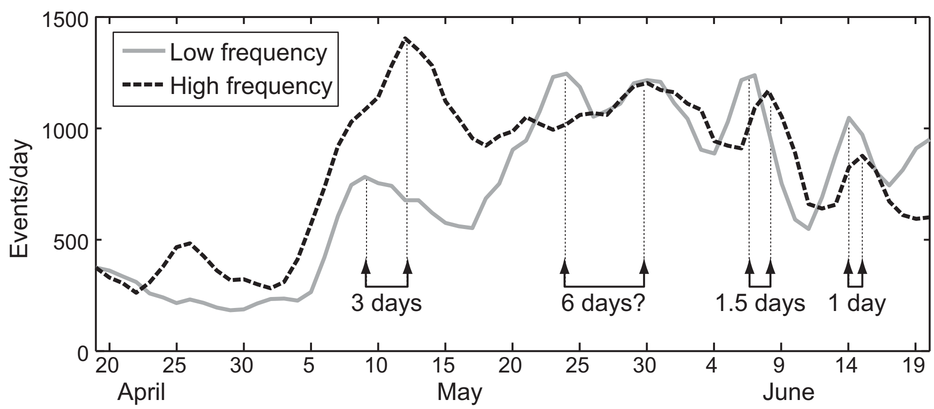

Figure 3. Time history of high- and low-frequency events at Bering Glacier. Vertical arrows mark apparent time lag between peaks in event classes.

weeks, the rate of each type of event modulates out of sync with the other. There is a suggestion that increases in low-frequency events are mirrored in the following days by increases in high-frequency events. This pattern is observed three to four times with lag times ranging from one to six days. The simplest interpretation is that the low-frequency events are a manifestation of increased fluid flow within or beneath the glacier. Increased water pressure beneath the glacier leads to local decoupling of the ice from the bed. This decoupling is known to change the stress distribution (Amundson et al., 2006). The new stress regime increases deformation that is accommodated, in part, by large numbers of high-frequency icequakes. Robust source mechanisms, beyond the abilities of the Bering Glacier array, are needed to test this hypothesis. However, these data demonstrate that different styles of seismic activity become active and inactive on the scale of days and months. These separate modulations on a variety of time scales demonstrate the potential for using different styles of seismic signals to measure seasonal, meteorological, and climate effects on glaciers.

REFERENCES CITED

Amundson, J.M., Truffer, M., and Lüthi, M.P., 2006, Time-dependent basal stress conditions beneath Black Rapids Glacier, Alaska, inferred from measurements of ice deformation and surface motion: Journal of Glaciology, v. 52, p. 347–357, doi: 10.3189/172756506781828593.

Amundson, J.M., Truffer, M., Lüthi, M.P., Fahnestock, M., West, M., and Motyka, R.J., 2008, Glacier, fjord, and seismic response to recent large calving events, Jakobshavn Isbræ, Greenland: Geophysical Research Letters, v. 35, L22501, doi: 10.1029/2008GL035281.

Anandakrishnan, S., and Alley, R.B., 1994, Ice stream C, Antarctica, sticky-spots detected by microearthquake monitoring: Annals of Glaciology, v. 20, p. 183–186.

Anandakrishnan, S., and Bentley, C.R., 1993, Microearthquakes beneath ice streams B & C, West Antarctica: Observations and implications: Journal of Glaciology, v. 39, p. 455–462.

Buurman, H., and West, M., 2010, Seismic precursors to explosive eruptions during the 2006 eruption of Augustine Volcano, Alaska, *in* Power, J., et al., eds., Investigations following the 2006 eruption of Augustine Volcano, Alaska: U.S. Geological Survey Professional Paper 1769 (in press).

Chouet, B.A., 1996, Long-period volcano seismicity: Its source and use in eruption forecasting: Nature, v. 380, p. 309–316, doi: 10.1038/380309a0.

Conway, H., Smith, B., Vaswani, P., Matsuoka, K., Rignot, E., and Claus, P., 2009, A low-frequency ice-penetrating radar system adapted for use from an airplane: Test results from Bering and Malaspina Glaciers, Alaska, USA: Annals of Glaciology, v. 50, p. 93–97, doi: 10.3189/172756409789097487.

Deichmann, N., Ansorge, J., and Rothlisberger, H., 1979, Observations of glacier seismicity on Unteraargletscher: Journal of Glaciology, v. 23, p. 409.

Ekström, G., Nettles, M., and Abers, G.A., 2003, Glacial earthquakes: Science, v. 302, p. 622–624, doi: 10.1126/science.1088057.

Ekström, G., Nettles, M., and Tsai, V.C., 2006, Seasonality and increasing frequency of Greenland glacial earthquakes: Science, v. 311, p. 1756–1758, doi: 10.1126/science.1122112.

Fujita, E., and Ida, Y., 2003, Geometrical effects and low-attenuation resonance of volcanic fluid inclusions for the source mechanism of long-period earthquakes: Journal of Geophysical Research, v. 108, no. B2, 2118, doi: 10.1029/2002JB001806.

Julian, B.R., 1994, Volcanic tremor: Nonlinear excitation by fluid flow: Journal of Geophysical Research, v. 99, p. 11,859–11,877, doi: 10.1029/93JB03129.

Julian, B.R., Miller, A.D., and Foulger, G.R., 1997, Non-double-couple earthquake mechanisms at the Hengill-Grensdalur volcanic complex, southwest Iceland: Geophysical Research Letters, v. 24, p. 743–746, doi: 10.1029/97GL00499.

Larsen, C.F., Truffer, M., LeBlanc, L., O'Neel, S., and West, M., 2007, Continuous measurements of ice motion and associated seismicity at Bering Glacier, Alaska: Eos (Transactions, American Geophysical Union), v. 88, abs. G33B-1232.

McNutt, S.R., 2002, Volcano seismology, *in* Lee, W.H.K., et al., eds., International handbook of earthquake and engineering seismology Volume 81: Palo Alto, California, International Association of Seismology and Physics of the Earth's Interior, p. 383–406.

McNutt, S.R., 2005, Volcanic seismology: Annual Review of Earth and Planetary Sciences, v. 33, p. 461–491, doi: 10.1146/annurev.earth.33.092203.122459.

Métaxian, J.-P., Araujo, S., Mora, M., and Lesage, P., 2003, Seismicity related to the glacier of Cotopaxi Volcano, Ecuador: Geophysical Research Letters, v. 30, 1483, doi: 10.1029/2002GL016773.

Molnia, B.F., and Post, A., 1995, Holocene history of Bering Glacier, Alaska—A prelude to the 1993–1994 surge: Physical Geography, v. 16, p. 87–117.

Nakano, M., Kumagai, H., Kumazawa, M., Yamaoka, K., and Chouet, B.A., 1998, The excitation and characteristic frequency of the long period volcanic event: An approach based on an inhomogeneous autoregressive model of a linear dynamic system: Journal of Geophysical Research, v. 103, p. 10,031–10,046.

Neave, K.G., and Savage, J.C., 1970, Icequakes on Athabasca Glacier: Journal of Geophysical Research, v. 75, p. 1351–1362, doi: 10.1029/JB075i008p01351.

Nettles, M.N., and 12 others, 2008, Step-wise changes in glacier flow speed coincide with calving and glacial earthquakes at Helheim Glacier, Greenland: Geophysical Research Letters, v. 35, L24503, doi: 10.1029/2008GL036127.

Neuberg, J., and O'Gorman, C., 2002, A model of the seismic wavefield in gas-charged magma: Application to Soufrière Hills Volcano, Montserrat, *in* Druitt, T.H., and Kokelaar, B.P., eds., The eruption of Soufriere Hills Volcano, Montserrat, from 1995 to 1999: Geological Society of London Memoir 21, p. 603–609.

Neuberg, J., Luckett, R., Baptie, B., and Olsen, K., 2000, Models of tremor and low-frequency earthquake swarms on Montserrat: Journal of Volcanology and Geothermal Research, v. 101, p. 83–104, doi: 10.1016/S0377-0273(00)00169-4.

O'Neel, S., and Pfeffer, W.T., 2007, Source mechanics for monochromatic icequakes produced during iceberg calving at Columbia Glacier, AK: Geophysical Research Letters, v. 34, L22502, doi: 10.1029/2007GL031370.

Qamar, A., 1988, Calving icebergs: A source of low-frequency seismic signals from Columbia Glacier, Alaska: Journal of Geophysical Research, v. 93, p. 6615–6623, doi: 10.1029/JB093iB06p06615.

Roman, D.C., Neuberg, J., and Luckett, R.R., 2006, Assessing the likelihood of volcanic eruption through analysis of volcanotectonic earthquake fault-plane solutions: Earth and Planetary Science Letters, v. 248, p. 244–252, doi: 10.1016/j.epsl.2006.05.029.

Smith, A.M., 2006, Microearthquakes and subglacial conditions: Geophysical Research Letters, v. 33, L24501, doi: 10.1029/2006GL028207.

St. Lawrence, W., and Qamar, A., 1979, Hydraulic transients: A seismic source in volcanoes and glaciers: Science, v. 203, p. 654–656, doi: 10.1126/science.203.4381.654.

Stuart, G., Murray, T., Brisbourne, A., Styles, P., and Toon, S., 2005, Seismic emissions from a surging glacier: Bakaninbreen, Svalbard: Annals of Glaciology, v. 42, p. 151–157, doi: 10.3189/172756405781812538.

Van der Veen, C.J., 1998, Fracture mechanics approach to penetration of surface crevasses on glaciers: Cold Regions Science and Technology, v. 27, p. 31–47.

Van Wormer, D., and Berg, E., 1973, Seismic evidence for glacier motion: Journal of Glaciology, v. 12, p. 259–265.

Walter, F., Deichmann, N., and Funk, M., 2008, Basal icequakes during changing subglacial water pressures beneath Gornergletscher, Switzerland: Journal of Glaciology, v. 54, p. 511–521, doi: 10.3189/002214308785837110.

Weaver, C.S., and Malone, S.D., 1979, Seismic evidence for discrete glacier motion at the rock-ice interface: Journal of Glaciology, v. 23, p. 171–184.

Wiens, D.A., Anandakrishnan, S., Winberry, J.P., and King, M.A., 2008, Simultaneous teleseismic and geodetic observations of the stick-slip motion of an Antarctic ice stream: Nature, v. 453, p. 770–774, doi: 10.1038/nature06990.

Willis, I.C., 1995, Interannual variations in glacier motion—A review: Progress in Physical Geography, v. 19, p. 61–106, doi: 10.1177/030913339501900104.

Wolf, L.W., and Davies, J.N., 1986, Glacier-generated earthquakes from Prince William Sound, Alaska: Seismological Society of America Bulletin, v. 76, p. 367–379.

Manuscript received 10 August 2009
Revised manuscript received 25 October 2009
Manuscript accepted 27 October 2009

Printed in USA